Appendix-I

EDS Data for Nitrogen Profiling

As nitriding progresses, more and more nitrogen diffuses in to the surface region and nitrogen concentration gradient is developed from the surface to core region. The concentration of nitrogen being maximum at the surface and minimum at the end of diffusion zone. The peak value of nitrogen as well as its variation over depth have been determined using Energy Dispersive Spectrometer (EDS). The EDS results are shown here in the enclosed data sheets in Appendix-I for various categories of nitride specimens.

The EDS profiles enclosed are as under:

EDS profiles for plasma nitrided specimens with no white layer:

- Nitrogen profile of plasma nitrided specimens with no white layer: Location -1 (At surface)
- Nitrogen profile of plasma nitrided specimens with no white layer: Location -2 (In diffusion zone)
- Nitrogen profile of plasma nitrided specimens with no white layer: Location -3 (In diffusion zone)
- Nitrogen profile of plasma nitrided specimens with no white layer: Location -4 (At diffusion zone – core interface)

EDS profiles for plasma nitrided specimens with less than 10μm white layer:

- Nitrogen profile of plasma nitrided specimens with white layer thickness less than 10 microns: Location -1 (At surface)
- Nitrogen profile of plasma nitrided specimens with white layer thickness less than 10 microns: Location -2 (In diffusion zone)
- Nitrogen profile of plasma nitrided specimens with white layer thickness less than 10 microns: Location -3 (In diffusion zone)
- Nitrogen profile of plasma nitrided specimens with white layer thickness less than 10 microns: Location -4 (In diffusion zone)

EDS profiles for plasma nitrided specimens with more than 10 μm white layer:

- Nitrogen profile of plasma nitrided specimens with white layer thickness more than 10 microns: Location -1 (At surface)

- Nitrogen profile of plasma nitrided specimens with white layer thickness more than 10 microns: Location -2 (In diffusion zone)

- Nitrogen profile of plasma nitrided specimens with white layer thickness more than 10 microns: Location -3 (In diffusion zone)

- Nitrogen profile of plasma nitrided specimens with white layer thickness more than 10 microns: Location -4 (In diffusion zone)

- Nitrogen profile of plasma nitrided specimens with white layer thickness more than 10 microns: Location -5 (At diffusion zone – core interface)

Nitrogen profile of plasma nitrided specimens with no white layer: Location -1 (At surface)

Spectrum processing :
No peaks omitted

Processing option : All elements analyzed (Normalised)
Number of iterations = 3

Standard :
N Not defined 1-Jun-1999 12:00 AM
Si SiO2 1-Jun-1999 12:00 AM
Cr Cr 1-Jun-1999 12:00 AM
Mn Mn 1-Jun-1999 12:00 AM
Fe Fe 1-Jun-1999 12:00 AM
Ni Ni 1-Jun-1999 12:00 AM
Mo Mo 1-Jun-1999 12:00 AM

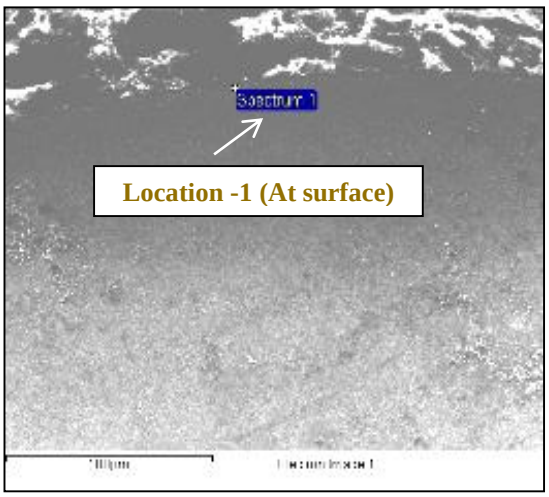

Element	Weight%	Atomic%
N K	5.89	19.89
Si K	0.61	1.03
Cr K	1.34	1.22
Mn K	0.84	0.72
Fe K	89.22	75.60
Ni K	1.58	1.27
Mo L	0.52	0.26
Totals	100.00	

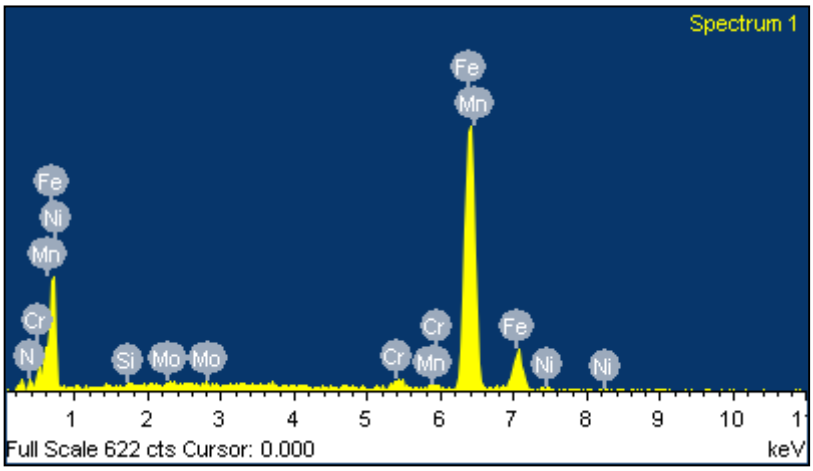

Nitrogen profile of plasma nitrided specimens with no white layer: Location -2 (In diffusion zone)

Spectrum processing :
No peaks omitted

Processing option : All elements analyzed (Normalised)
Number of iterations = 3

Standard :
N Not defined 1-Jun-1999 12:00 AM
Si SiO2 1-Jun-1999 12:00 AM
Cr Cr 1-Jun-1999 12:00 AM
Mn Mn 1-Jun-1999 12:00 AM
Fe Fe 1-Jun-1999 12:00 AM
Ni Ni 1-Jun-1999 12:00 AM
Mo Mo 1-Jun-1999 12:00 AM

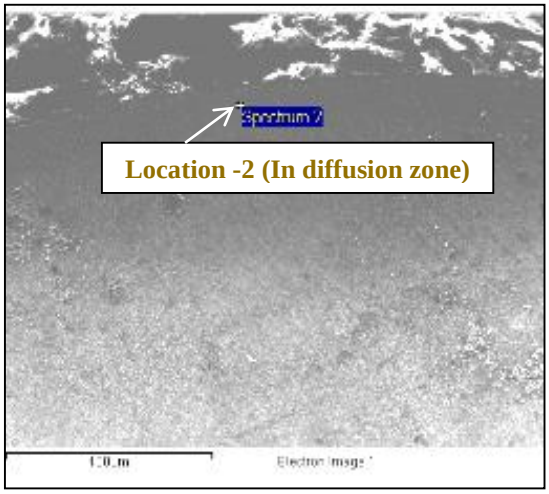

Element	Weight%	Atomic%
N K	3.48	12.52
Si K	0.51	0.92
Cr K	1.23	1.19
Mn K	1.14	1.04
Fe K	92.21	83.13
Ni K	1.34	1.15
Mo L	0.10	0.05
Totals	100.00	

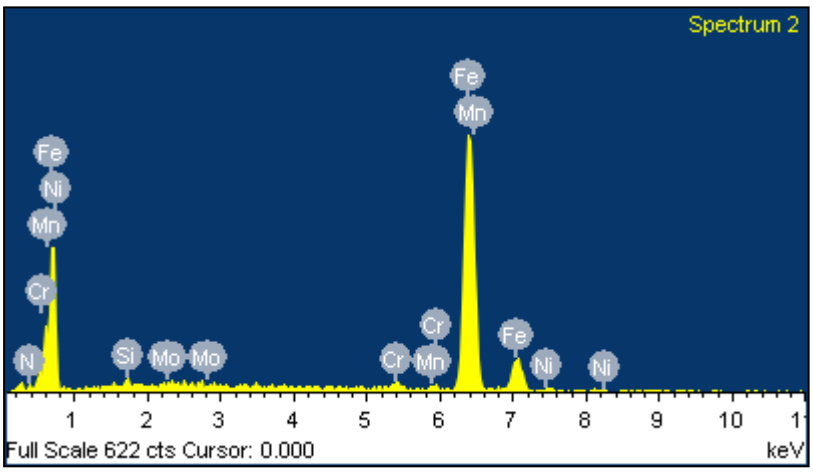

Nitrogen profile of plasma nitrided specimens with no white layer: Location -3 (In diffusion zone)

Spectrum processing :
No peaks omitted

Processing option : All elements analyzed (Normalised)
Number of iterations = 2

Standard :
N Not defined 1-Jun-1999 12:00 AM
Si SiO2 1-Jun-1999 12:00 AM
Cr Cr 1-Jun-1999 12:00 AM
Mn Mn 1-Jun-1999 12:00 AM
Fe Fe 1-Jun-1999 12:00 AM
Ni Ni 1-Jun-1999 12:00 AM
Mo Mo 1-Jun-1999 12:00 AM

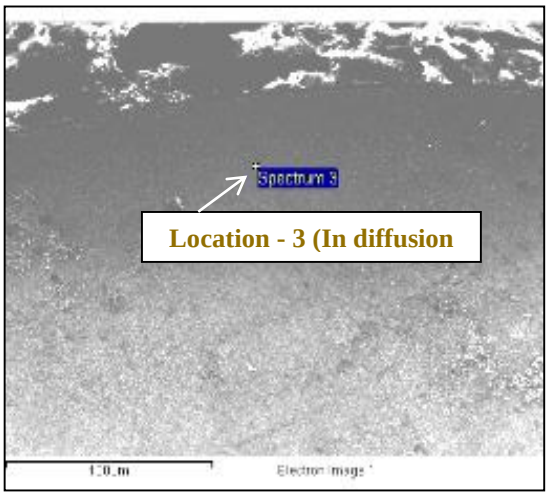

Element	Weight%	Atomic%
N K	1.11	4.27
Si K	0.70	1.35
Cr K	1.55	1.61
Mn K	1.01	0.99
Fe K	94.21	90.77
Ni K	0.64	0.59
Mo L	0.77	0.43
Totals	100.00	

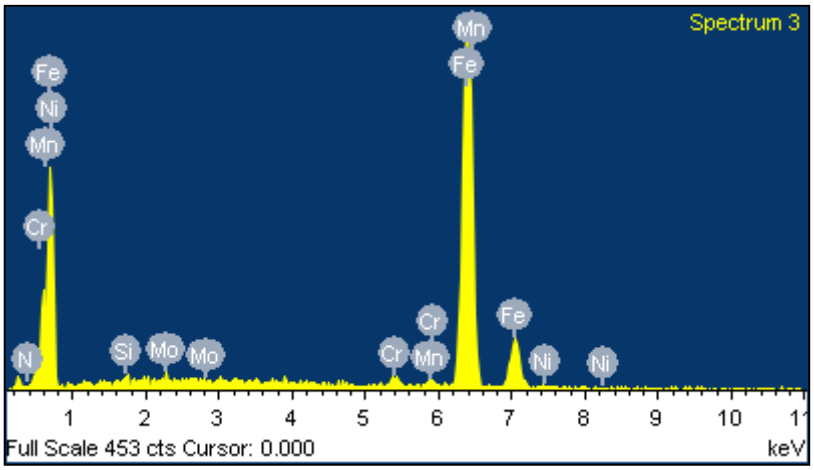

Nitrogen profile of plasma nitrided specimens with no white layer: Location -4 (At diffusion zone – core interface)

Spectrum processing :
No peaks omitted

Processing option : All elements analyzed (Normalised)
Number of iterations = 2

Standard :
N Not defined 1-Jun-1999 12:00 AM
Si SiO2 1-Jun-1999 12:00 AM
Cr Cr 1-Jun-1999 12:00 AM
Mn Mn 1-Jun-1999 12:00 AM
Fe Fe 1-Jun-1999 12:00 AM
Ni Ni 1-Jun-1999 12:00 AM
Mo Mo 1-Jun-1999 12:00 AM

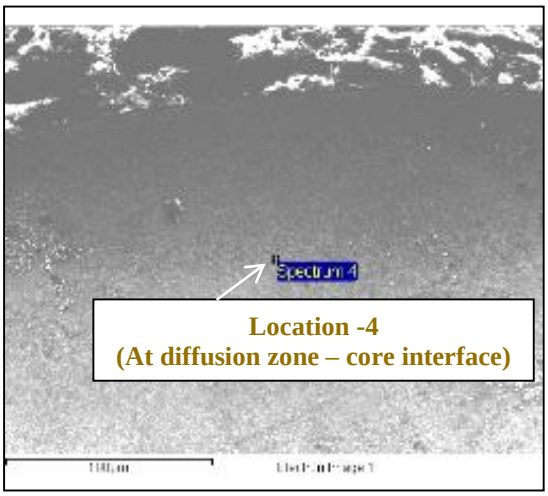

Element	Weight%	Atomic%
N K	0.10	0.40
Si K	0.58	1.15
Cr K	1.56	1.67
Mn K	0.73	0.74
Fe K	93.54	93.25
Ni K	2.08	1.97
Mo L	1.42	0.82
Totals	100.00	

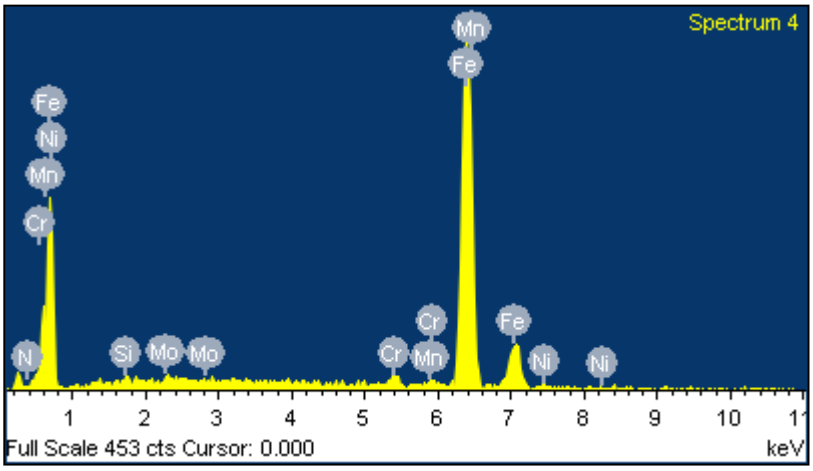

Nitrogen profile of plasma nitrided specimens with white layer thickness less than 10 microns: Location -1 (At surface)

Spectrum processing :
No peaks omitted

Processing option : All elements analyzed (Normalised)
Number of iterations = 3

Standard :
N Not defined 1-Jun-1999 12:00 AM
Si SiO2 1-Jun-1999 12:00 AM
Cr Cr 1-Jun-1999 12:00 AM
Mn Mn 1-Jun-1999 12:00 AM
Fe Fe 1-Jun-1999 12:00 AM
Ni Ni 1-Jun-1999 12:00 AM
Mo Mo 1-Jun-1999 12:00 AM

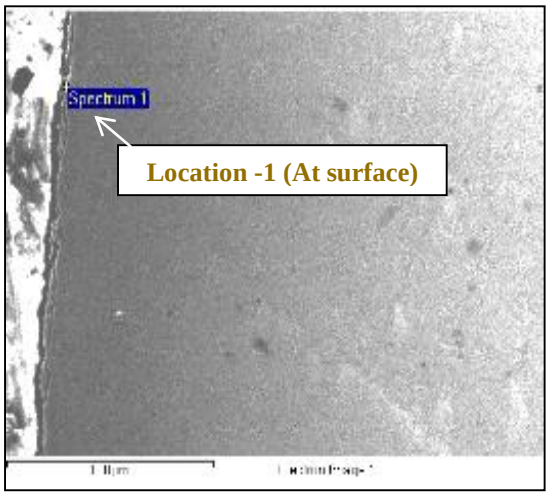

Element	Weight%	Atomic%
N K	8.22	26.24
Si K	0.46	0.73
Cr K	0.52	0.45
Mn K	0.63	0.51
Fe K	88.64	70.97
Ni K	1.32	1.01
Mo L	0.21	0.10
Totals	100.00	

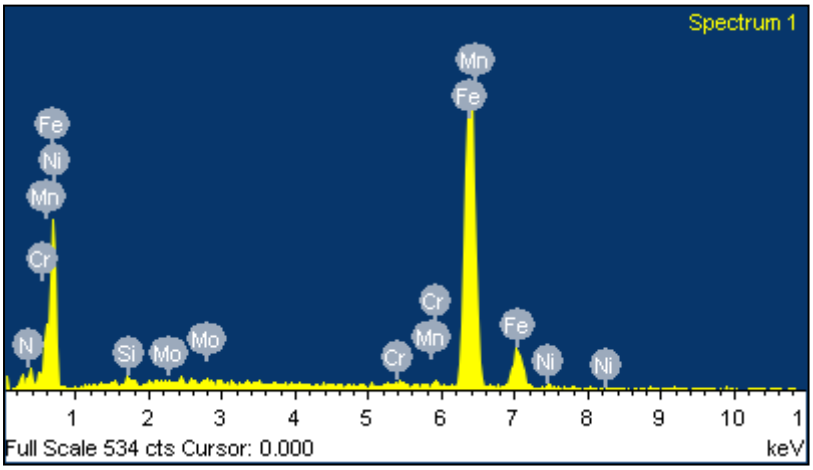

Nitrogen profile of plasma nitrided specimens with white layer thickness less than 10 microns: Location -2 (In diffusion zone)

Spectrum processing :
No peaks omitted

Processing option : All elements analyzed (Normalised)
Number of iterations = 3

Standard :
N Not defined 1-Jun-1999 12:00 AM
Si SiO2 1-Jun-1999 12:00 AM
Cr Cr 1-Jun-1999 12:00 AM
Mn Mn 1-Jun-1999 12:00 AM
Fe Fe 1-Jun-1999 12:00 AM
Ni Ni 1-Jun-1999 12:00 AM

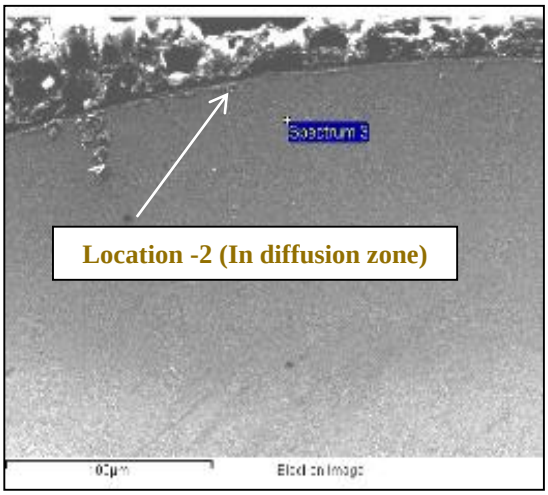

Element	Weight%	Atomic%
N K	2.35	8.71
Si K	0.48	0.90
Cr K	1.19	1.19
Mn K	1.15	1.08
Fe K	92.33	85.90
Ni K	2.51	2.22
Totals	100.00	

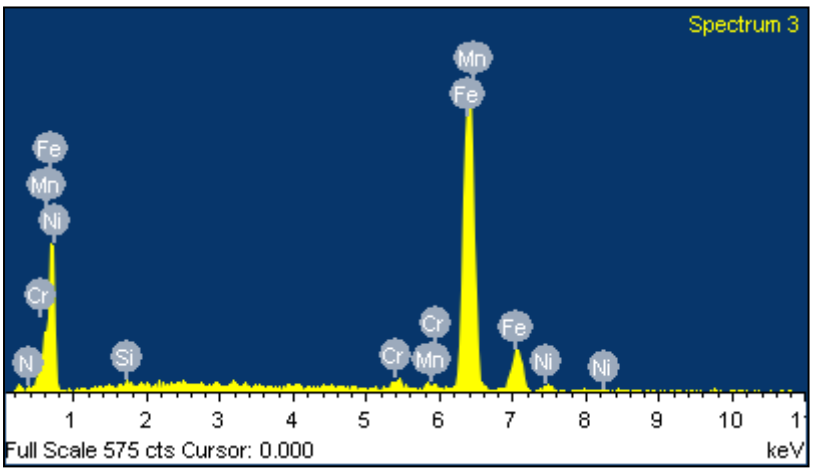

Nitrogen profile of plasma nitrided specimens with white layer thickness less than 10 microns: Location -3 (In diffusion zone)

Spectrum processing :
No peaks omitted

Processing option : All elements analyzed (Normalised)
Number of iterations = 2

Standard :
N Not defined 1-Jun-1999 12:00 AM
Si SiO2 1-Jun-1999 12:00 AM
Cr Cr 1-Jun-1999 12:00 AM
Mn Mn 1-Jun-1999 12:00 AM
Fe Fe 1-Jun-1999 12:00 AM
Ni Ni 1-Jun-1999 12:00 AM

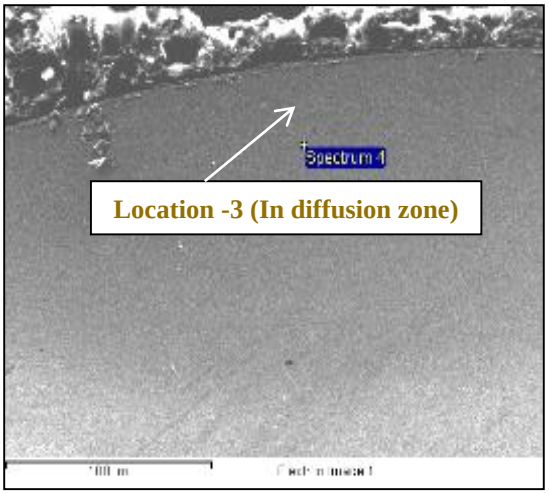

Element	Weight%	Atomic%
N K	0.75	2.89
Si K	0.62	1.19
Cr K	1.46	1.53
Mn K	0.69	0.68
Fe K	95.54	92.84
Ni K	0.95	0.87
Totals	100.00	

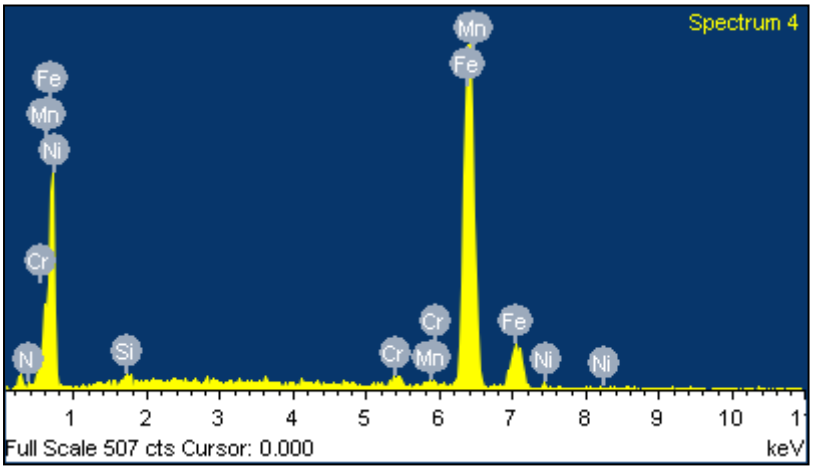

Nitrogen profile of plasma nitrided specimens with white layer thickness less than 10 microns: Location - 4 (At diffusion zone – core interface)

Spectrum processing :
No peaks omitted

Processing option : All elements analyzed (Normalised)
Number of iterations = 2

Standard :
N Not defined 1-Jun-1999 12:00 AM
Si SiO2 1-Jun-1999 12:00 AM
Cr Cr 1-Jun-1999 12:00 AM
Mn Mn 1-Jun-1999 12:00 AM
Fe Fe 1-Jun-1999 12:00 AM
Ni Ni 1-Jun-1999 12:00 AM
Mo Mo 1-Jun-1999 12:00 AM

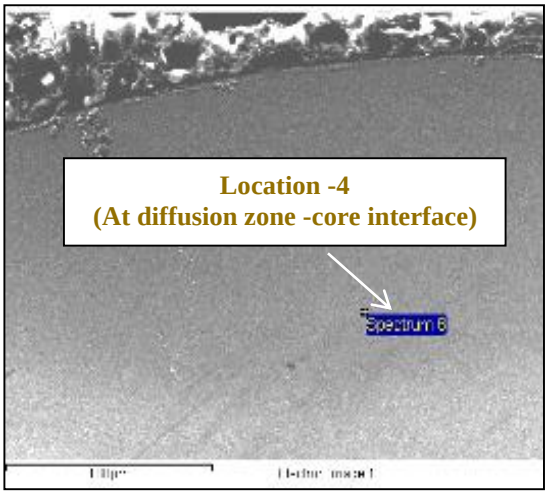

Element	Weight%	Atomic%
N K	0.29	1.15
Si K	0.79	1.55
Cr K	1.24	1.31
Mn K	0.69	0.70
Fe K	95.85	94.48
Ni K	0.46	0.43
Mo L	0.67	0.38
Totals	100.00	

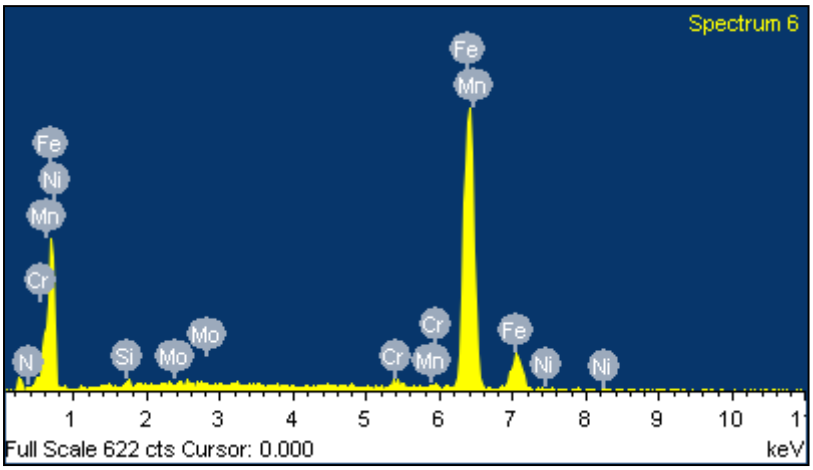

Nitrogen profile of plasma nitrided specimens with white layer thickness more than 10 microns: Location -1 (At surface)

Spectrum processing :
No peaks omitted

Processing option : All elements analyzed (Normalised)
Number of iterations = 3

Standard :
N Not defined 1-Jun-1999 12:00 AM
Si SiO2 1-Jun-1999 12:00 AM
Cr Cr 1-Jun-1999 12:00 AM
Mn Mn 1-Jun-1999 12:00 AM
Fe Fe 1-Jun-1999 12:00 AM
Ni Ni 1-Jun-1999 12:00 AM

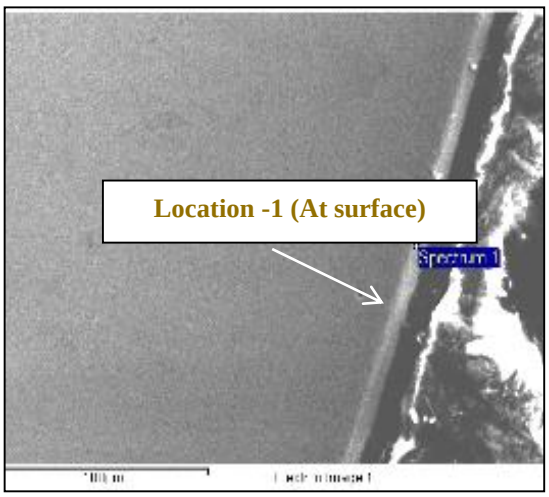

Element	Weight%	Atomic%
N K	8.22	26.24
Si K	0.46	0.73
Cr K	0.52	0.45
Mn K	0.63	0.51
Fe K	88.64	70.97
Ni K	1.32	1.01
Mo L	0.21	0.10
Totals	100	

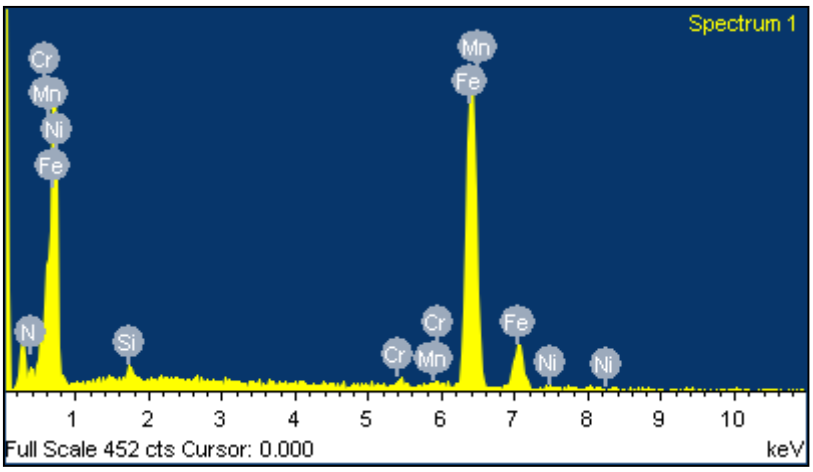

Nitrogen profile of plasma nitrided specimens with white layer thickness more than 10 microns: Location -2 (In diffusion zone)

Spectrum processing :
No peaks omitted

Processing option : All elements analyzed (Normalised)
Number of iterations = 3

Standard :
N Not defined 1-Jun-1999 12:00 AM
Si SiO2 1-Jun-1999 12:00 AM
Cr Cr 1-Jun-1999 12:00 AM
Mn Mn 1-Jun-1999 12:00 AM
Fe Fe 1-Jun-1999 12:00 AM
Ni Ni 1-Jun-1999 12:00 AM
Mo Mo 1-Jun-1999 12:00 AM

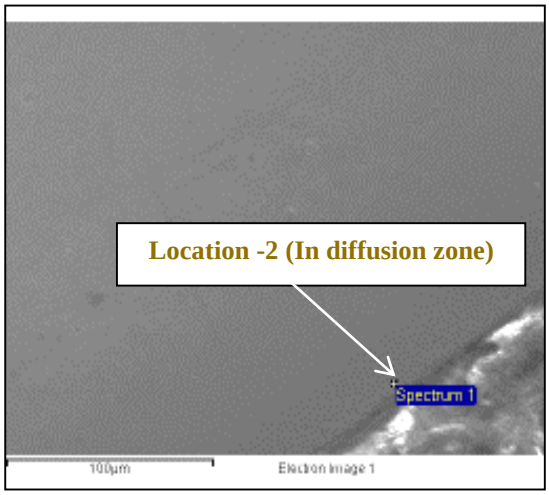

Element	Weight%	Atomic%
N K	5.12	17.61
Si K	0.62	1.07
Cr K	1.85	1.72
Mn K	0.42	0.37
Fe K	90.57	78.19
Ni K	1.06	0.87
Mo L	0.36	0.18
Totals	100.00	

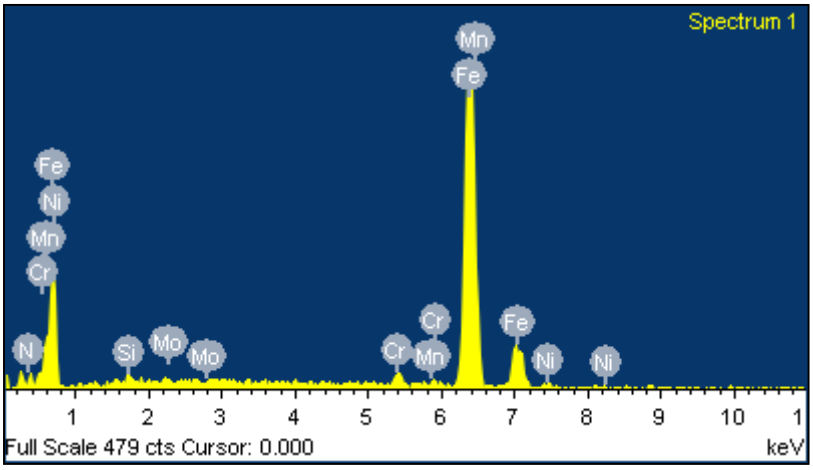

Nitrogen profile of plasma nitrided specimens with white layer thickness more than 10 microns: Location -3 (In diffusion zone)

Spectrum processing :
No peaks omitted

Processing option : All elements analyzed (Normalised)
Number of iterations = 3

Standard :
N Not defined 1-Jun-1999 12:00 AM
Si SiO2 1-Jun-1999 12:00 AM
Cr Cr 1-Jun-1999 12:00 AM
Mn Mn 1-Jun-1999 12:00 AM
Fe Fe 1-Jun-1999 12:00 AM
Ni Ni 1-Jun-1999 12:00 AM
Mo Mo 1-Jun-1999 12:00 AM

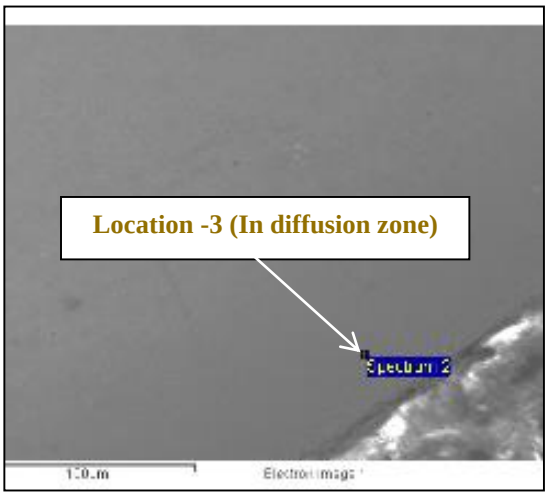

Element	Weight%	Atomic%
N K	2.21	8.28
Si K	0.64	1.20
Cr K	1.38	1.39
Mn K	0.94	0.89
Fe K	92.37	86.62
Ni K	0.82	0.73
Mo L	1.64	0.89
Totals	100.00	

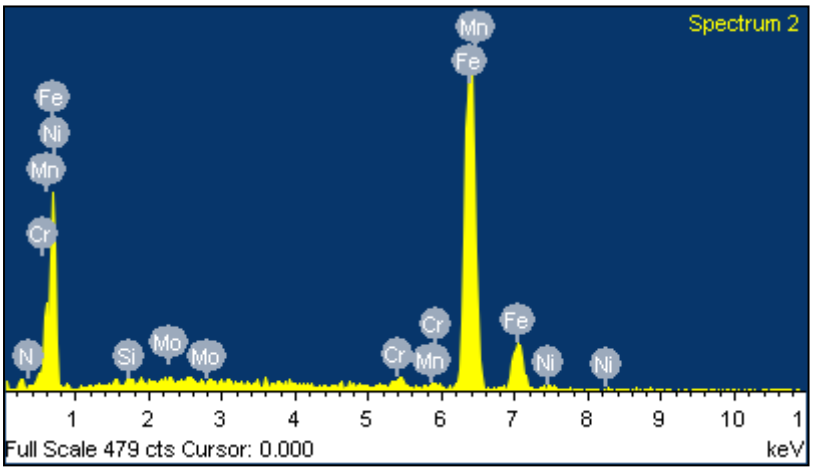

Nitrogen profile of plasma nitrided specimens with white layer thickness more than 10 microns: Location -4 (In diffusion zone)

Spectrum processing :
No peaks omitted

Processing option : All elements analyzed (Normalised)
Number of iterations = 2

Standard :
N Not defined 1-Jun-1999 12:00 AM
Si SiO2 1-Jun-1999 12:00 AM
Cr Cr 1-Jun-1999 12:00 AM
Mn Mn 1-Jun-1999 12:00 AM
Fe Fe 1-Jun-1999 12:00 AM
Ni Ni 1-Jun-1999 12:00 AM
Mo Mo 1-Jun-1999 12:00 AM

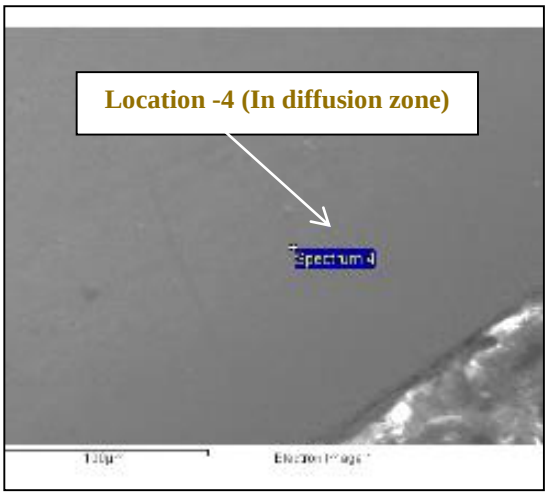

Element	Weight%	Atomic%
N K	1.03	3.96
Si K	0.67	1.28
Cr K	1.96	2.03
Mn K	0.50	0.49
Fe K	94.12	90.77
Ni K	1.41	1.30
Mo L	0.31	0.17
Totals	100.00	

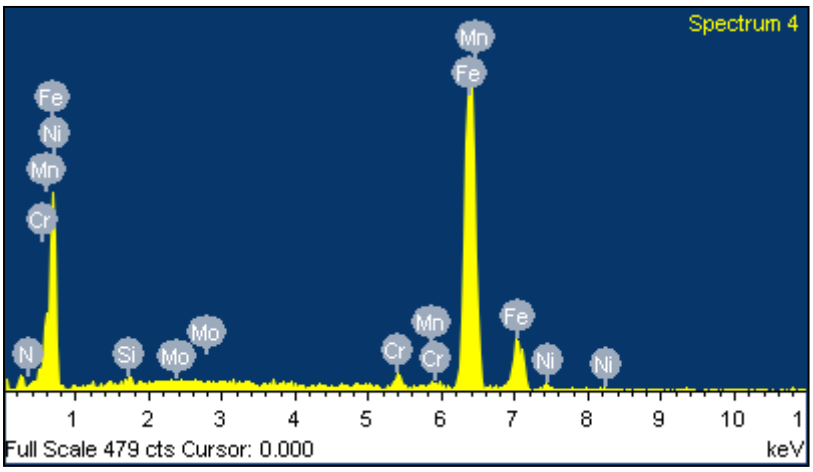

Nitrogen profile of plasma nitrided specimens with white layer thickness more than 10 microns: Location -5 (At diffusion zone – core interface)

Spectrum processing :
No peaks omitted

Processing option : All elements analyzed (Normalised)
Number of iterations = 2

Standard :
N Not defined 1-Jun-1999 12:00 AM
Si SiO2 1-Jun-1999 12:00 AM
Cr Cr 1-Jun-1999 12:00 AM
Mn Mn 1-Jun-1999 12:00 AM
Fe Fe 1-Jun-1999 12:00 AM
Ni Ni 1-Jun-1999 12:00 AM

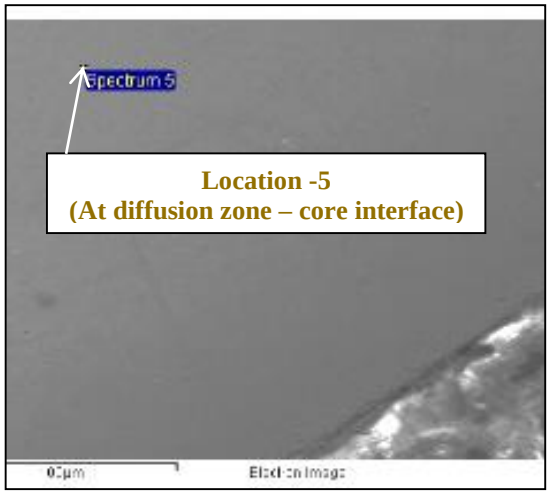

Element	Weight%	Atomic%
N K	0.10	0.41
Si K	0.48	0.94
Cr K	0.73	0.78
Mn K	0.98	0.99
Fe K	95.12	94.44
Ni K	2.58	2.44
Totals	100.00	

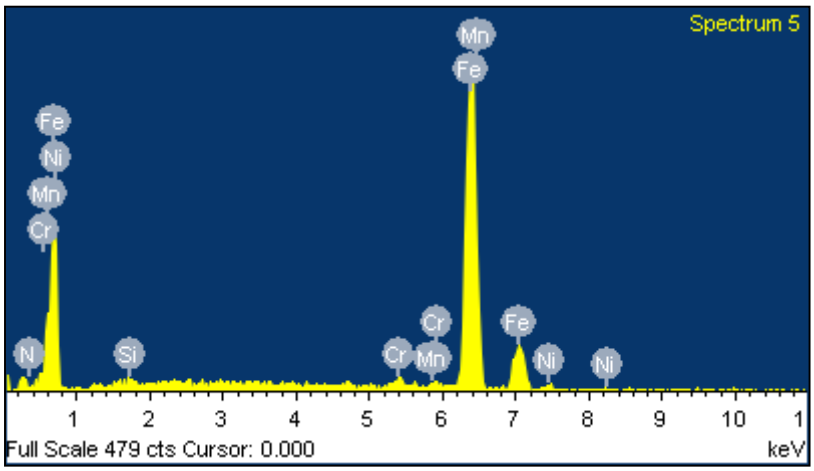

Appendix-II

Sample calculations and Data on Fatigue Analysis

II-1. Derivation of Formulae Used for Fatigue Data Analysis:

Formulae used for analysis of fatigue data have been derived in the following sections:

II-1-A. Derived parameters for S-N curves (i.e. N_f Derived):

The purpose here is to convert (N_f experimental) to (N_f Derived) to enable to plot S-N curves. As the fatigue data follows a power law relationship it can be expressed as –

$$\sigma_\alpha = \alpha\left(N_f\right)^\beta \quad (1)$$

Where:

σ_α = Alternating stress (stress amplitude)

N_f = Number of cycles to failure

α, β = Basquin pre-exponent and fatigue life exponent, respectively

The estimation for α and β is carried out by first linearizing equation (1) as:

$$\ln \sigma_\alpha = ln\ \left(\alpha\left[N_f^\beta\right]\right) \quad (2)$$

$$= ln\ \alpha + \beta\ \ ln\ N_f \quad (3)$$

Taking $ln\ \ \sigma_a$ as variable y and $ln\ N_f$ as variable x, the above equation takes the familiar form of a straight line

$$y = a + bx \quad (4)$$

Where,

$$y = ln\ \sigma_a$$

$$a\ (intercept) = ln\ \alpha$$

$$b\ (slope) = \beta$$

$$x = ln\ \ N_f$$

From Eqs. (3) and (4), the values of a and b are estimated using minimal variance "regression" estimators as

$$\hat{a} = ln\ \hat{\alpha} = \frac{[\sum_{i=1}^{N} Y_i] - [\hat{f}(\sum_{i=1}^{N} X_i)]}{N} \tag{5}$$

$$\hat{b} = \frac{\sum_{i=1}^{N} X_i Y_i - \frac{(\sum_{i=1}^{N} X_i)(\sum_{i=1}^{N} Y_i)}{N}}{(\sum_{i=1}^{N} X_i^2) - \frac{(\sum_{i=1}^{N} X_i)^N}{N}} \tag{6}$$

The coefficient of determination R^2 is computed to quantify the accuracy of the estimate. This is given as:

$$R^2 = \frac{SS_R}{SS_T} = 1 - \frac{SS_{Req}}{SS_T} \tag{7}$$

With $O \leq R^2 \leq 1$

Where

$$SS_T = SS_{Res} + SS_R \tag{8}$$

and

$$SS_T = \sum_{i=1}^{N} (Y_i - \bar{Y})^2$$

$$SS_{Req} = \sum_{i=1}^{N} \left(Y_1 - \hat{Y}_1\right)^2$$

$$SS_R = \sum_{i=1}^{N} \left(\hat{Y}_i - \hat{Y}\right)^2$$

$$\bar{Y} = \frac{\sum_{i=1}^{N} Y_i}{N}$$

From the estimators, the Basquin coefficients are estimated as:

$$\hat{\alpha} = exp[\hat{a}]$$

$$\hat{\beta} = \hat{b} \quad (9)$$

This enables deriving the estimated Basquin model as:

$$\hat{\sigma}_a = \hat{\alpha}\left(N_f\right)^{\hat{\beta}} \quad (10a)$$

$$= exp[\hat{a}]\left(N_f\right)^{\hat{b}} \quad (10b)$$

II-1-B. Fatigue stress modification factor, $(\theta_{coat})_I$:

The aim is to develop a factor which expresses ratio between the bending stress that can be applied for the specimen of a particular surface treatment to the stress for an base material/untreated specimen for a given number of fatigue life cycles. Hence, a ratio of stresses for these two treatments is determined by taking a simple ratio of the estimated Basquin relationship for the i[th] treatment to the estimated Basquin relationship to the base material as follow:

$$(\theta_{coat})_i = \frac{(\sigma_\alpha)_i}{(\sigma_{a\alpha})_b} = \frac{\alpha(N_f)^{\beta_1}}{\alpha(N_f)^{\beta_2}} = \left[\frac{\alpha_i}{\alpha_b}\right]\left[N_f^{(\beta_i\beta_o)}\right] = \theta_{PEt}N_f^{\theta_{Ei}} \quad (11)$$

Where:

i = i[th] treatment category

b = Base material

$\alpha_i\alpha_b$ = Basquin pre-exponent for i[th] treatment and base material categories, respectively

$\beta_i\beta_b$ = Basquin exponent for i[th] treatment and base material categories, respectively

$\theta_{PEi}, \theta_{Ei}$ = Life reduction pre-exponent and exponent, respectively for treatment i

II-1-C. Cycle modification factor, Ψ_1 :

Cycle modification factor, Ψ_1 is a factor which expresses ratio between number of fatigue cycles that a particular surface treatment can withstand to the number of cycles withstood by a base material/untreated specimen for a applied stress level. The cycle modification factor for i[th] surface treatment is derived by first inverting the Basquin relationships as shown below:

$$\hat{\sigma}_{ai} = exp[\hat{a}_i]\left(N_f\right)^{\hat{b}_i} \quad (12)$$

$$\text{as } \left(N_f\right)_i = (\hat{\sigma}_{ai})^{\frac{1}{\hat{b}_i}}_{n_i} exp\left[-\frac{\hat{a}_i}{\hat{b}_i}\right] \quad (13)$$

$$= \varepsilon_i[\hat{\sigma}_a]^{n_i} \quad (14)$$

$$\text{and } \left(N_f\right)_b = (\sigma_{ab})^{\frac{1}{\hat{b}_b}} exp\left[-\frac{\hat{a}_b}{\hat{b}_b}\right] \quad (15)$$

$$= \varepsilon_b(\sigma_a)^{n_b} \quad (16)$$

Subsequently, ratio of Eqs. (13) and (16) give:

$$\frac{(N_f)_i}{(N_f)_b} = \Psi_{\mathrm{i}} = \frac{\xi_{\mathrm{i}}(\sigma_\alpha)^{\mathrm{n_i}}}{\xi_{\mathrm{b}}(\sigma_\alpha)^{\mathrm{n_b}}} = \left[\frac{\xi_{\mathrm{i}}}{\xi_{\mathrm{b}}}\right]\left[\sigma_\alpha^{(\mathrm{n_i n_b})}\right] = \Psi_{\mathrm{PEi}}\sigma_\alpha^{\Psi_{\mathrm{PEi}}} \quad (17)$$

Where,

i = i[th] treatment category

b = base material category

ξ_b, ξ_i = Inverse Basquin pre-exponent for base material and i[th] categories, respectively

η_b, η_i = Inverse Basquin exponents for base material and i[th] categories, respectively

$\Psi_{\mathrm{PEi}}\Psi_{\mathrm{Ei}}$ = Cycle modification pre-exponent and exponent, respectively for i[th] treatment

II-2-A. Sample Calculation using Formulae Derived for Fatigue Data Analysis:

A sample calculation for plasma nitriding treatment (with compound/white layer thickness of less than 10 microns) has been shown here.

The treatment has been identified as "PN" for the purpose of this calculation. Other nomenclatures used are:

σ_α = Alternating stress (stress amplitude)

N_f = Number of cycles to failure for "PN" treatment

α_{PN} & α_b = Basquin pre-exponent for "PN" treatment and base material categories, respectively

β_{PN} & β_b = Basquin exponent for "PN" and base material categories, respectively

Sample Calculation for Derived parameters for S-N curves:

Table 1 below shows fatigue test results of fatigue life cycles obtained for the various bending stresses applied for PN treatment. These values have been taken for solving the deriving Basquin parameters.

Table II.1: Fatigue life cycles data of Plasma nitrided category (with less than 10 microns)

Bending stress applied, σ_α	Fatigue life cycles, N_f
697.7	3.98E+07
767.5	7.11E+06
837.2	4.36E+06
907.0	4.08E+05
976.8	3.52E+04
1255.9	6.50E+03

For the purpose of converting data in Equation No. 3 of Annexure-I, the above values were converted in ln (i.e. Log to the base e) as shown in Table II.2.

Table II.2: Fatigue results converted into Basquin relationship

$y = ln\ \sigma_a$	$x = ln\ N_f$
6.548	17.50
6.643	15.78
6.730	15.29
6.810	12.92
6.884	10.47
7.136	8.78

From the above data, values of intercept '*a*'and slope '*b'* were determined using equations for regression analysis in Microsoft Excel. The results obtained are:

Intercept, '*a*' (i.e. ln α_{PN}) = 7.58

Slope, '*b'* (i.e. β_{PN}) = - 0.059

This gives values of Basquin co-efficient α_{PN} & β_{PN} as follow:

$\alpha_{PN} = 1.958 \times 10^3$

β_{PN} = -0.059

Now, the relation between σ_a and N_f (Derived) is:

$\sigma_a = 1.958 \times 10^3 \times (N_f \text{ (Derived)})^{-0.059}$

On rewriting the above equation in terms of *Nf* (Derived) we get,

N_f(Derived) = $(\sigma_a / 1.958 \times 10^3)^{-1/0.059}$

Solving above equation for a value of bending stress σ_a = 697.7 MPa, we get,

N_f (Derived) = $(697.7/1958)^{-16.95}$

= 3.95E+07 cycles

Similarly for all other values of σ_α, corresponding values of N_f (Derived) can be obtained and the same has been given in Table II.3.

Table II.3: Derived fatigue life cycles using Basquin parameters

Stress,σ_α	Fatigue Life(Experimental), N_f	Fatigue Life($Derived$), N_f
697.7	3.98E+07	3.95E+07
767.5	7.11E+06	7.84E+06
837.2	4.36E+06	1.80E+06
907.0	4.08E+05	4.62E+05
976.8	3.52E+04	1.32E+05
1255.9	6.50E+03	1.86E+03

II-2-B. Sample Calculation for Fatigue Stress Modification factor, $(\theta_{coat})_{PN}$:

By taking the ratio of the estimated Basquin relationship for PN treatment to the estimated Basquin relationship of the base material, $(\theta_{coat})_{PN}$ can be written as:

$$(\theta_{coat})_{PN} = \left[\frac{\alpha_{PN}}{\alpha_b}\right]\left[N_f^{(\beta_{PN}\beta_b)}\right]$$

Where:

α_{PN} & α_b = Basquin pre-exponent for PN treatment and base material categories, respectively

β_{PN} & β_b = Basquin exponent for PN treatment and base material categories, respectively

On substituting the values of Basquin pre-exponent and exponents as given below in above equation,

$\alpha_{PN} = 1.958 \times 10^3$

$\alpha_b = 3.31 \times 10^3$

$\beta_{PN} = -0.059$

$\beta_b = -0.11$

the Equation for Fatigue Stress Modification factor, $(\theta_{coat})_{PN}$ can be written as:

$$(\theta_{coat})_{PN} = \frac{1.958\times10^3 Nf^{-0.059}}{3.31\times10^3 Nf^{-0.11}}$$

$$= 0.592\, Nf^{0.051}$$

Substituting the value of Nf= 3.95E+07 in above equation, one gets Fatigue Stress Modification factor as follows.

$$(\theta_{coat})_{PN} = 0.592 \text{ X } (3.95\text{E} + 07)^{0.051}$$
$$= 1.445$$

Similarly, for all other values of N_f, the corresponding values of $(\theta_{coat})_{PN}$ are calculated the results obtained are given in Table 4 below.

Table II.4: Stress Modification factors obtained through calculations

$\boldsymbol{Stress, \sigma_a}$	$\boldsymbol{Fatigue\ life\ cycles, Nf}$	**Stress Modification factors,** $\boldsymbol{(\theta_{coat})_{PN}}$
698	3.95E+07	1.445
768	7.84E+06	1.330
837	1.80E+06	1.234
907	4.62E+05	1.151
977	1.32E+05	1.080
1256	1.86E+03	0.869

II-2-C. Sample Calculation for Cycle modification factor, Ψ_{PN}

The cycle modification factor for PN surface treatment (Ψ_{PN}) is derived using formula,

$$\Psi_{PN} = \left[\frac{\xi_{PN}}{\xi_b}\right]\left[\sigma_\alpha^{(n_{PN} n_b)}\right]$$

Where,

ξ_b & ξ_{PN} = Inverse Basquin pre-exponent for base material and PN categories, respectively

η_b & η_{PN} = Inverse Basquin exponents for base material and PN categories, respectively

On substituting the values of Inverse Basquin pre-exponent and Inverse Basquin exponent as given below in above equation,

for $\alpha_{PN} = 1.958 \times 10^3$, the inverse value is $\xi_{PN} = 1/\alpha_{PN} = 1 / 1.958 \times 10^3$

$\alpha_b = 3.31 \times 10^3$, the inverse value is $\xi_b = 1/\alpha_b = 1 / 3.31 \times 10^3$

$\beta_{PN} = -0.059$, the inverse value is $\eta_{PN} = 1/\beta_{PN} = 1 / (-0.059) = -16.95$

$\beta_b = -0.11$, the inverse value is $\eta_b = 1/\beta_b = 1 / (-0.11) = -9.09$

the Equation for Cycle Modification factor, Ψ_{PN} can be written as:

$$\Psi_{PN} = \left[\frac{\xi_{PN}}{\xi_b}\right]\left[\sigma_\alpha^{(n_{PN} n_b)}\right]$$

$$= \frac{(3.31\times10^3)^{-9.091}}{(1.958\times10^3)^{-16.95}} 6a^{-7.859}$$

$$= \frac{1.003 \times 10^{-32}}{1.60 \times 10^{-56}} 6a^{-7.859}$$

$$= 6.27 \times 10^{23} 6a^{-7.859}$$

For a given value of $6a$ = 698 MPa

$\Psi_{PN} = 6.27 \times 10^{23}(698)^{-7.859}$

$= 27.4$

Substituting the value of Nf= 3.95E+07 in above equation, one gets Fatigue Stress Modification factor as follows.

Similarly, cycle modification factor, $\boldsymbol{\Psi_{PN}}$ are calculated for all other values of $6a$ and are given in Table 5 below:

Table II.5: Cycle Modification Factors obtained through calculations

$Stress, \sigma a$	Cycle Modification Factors, Ψ_{PN}
700	2.74E+01
800	9.59E+00
900	3.80E+00
1000	1.66E+00
1100	7.80E-01
1200	3.90E-01

Following is the summary of data on derived fatigue life cycles, stress modification factors and cycle modification factors for untreated and various surface treated specimens.

Derived values of fatigue life from Basquin exponents					
Applied stress, Mpa	**Untreated**	**Thermal spray-Alumina**	**P. N. (No C. L.)**	**P. N. (C. L. <10 micron)**	**P. N. (C. L. >10 micron)**
700	8.80E+05	3.940E+04		3.95E+07	3.54E+04
770	3.81E+05	2.910E+04		7.84E+06	2.30E+04
840	1.77E+05	2.200E+04	6.84E+08	1.80E+06	1.55E+04
910	8.78E+04	1.707E+04	3.52E+07	4.62E+05	1.07E+04
975	4.58E+04	1.348E+04	2.26E+06	1.32E+05	7.66E+03
1045			1.75E+05		
1115			1.61E+04		
Stress Modification factor vs Fatigue Life Cycles					
Cycles	**Chrome plated**	**P. N. (No C. L.)**	**P. N. (C.L. <10 micron)**	**P. N. (C.L. >10 Micron)**	**Untreated**
4.58E+04	0.89	1.0676	1.023	0.647	1.0
8.78E+04	0.7	1.1269	1.058	0.602	1.0
1.77E+05	0.53	1.1944	1.096	0.558	1.0
2.58E+05	0.46	1.232	1.118	0.535	1.0
3.81E+05	0.4	1.273	1.14	0.512	1.0
8.80E+05	0.29	1.364	1.19	0.467	1.0
2.76E+06	0.189	1.5	1.261	0.412	1.0
Cycle Modification Factors for Applied Stress					
Applied Stress, MPa	**Chrome plated**	**P. N. (No C. L.)**	**P. N. (C.L. <10 micron)**	**P. N. (C.L. >10 Micron)**	**Untreated**
200	8.40E-06	4.72E+20	5.17E+05	8.67E-05	1.0
300	1.46E-04	5.66E+15	2.13E+04	5.47E-04	1.0
400	1.11E-03	1.82E+12	2.23E+03	2.02E-03	1.0
500	5.37E-03	3.57E+09	3.85E+02	5.56E-03	1.0
600	1.94E-02	2.19E+07	9.20E+01	1.27E-02	1.0
700	5.76E-02	2.95E+05	2.74E+01	2.56E-02	1.0
800	1.47E-01	7.05E+03	9.59E+00	4.70E-02	1.0
900	3.39E-01	2.62E+02	3.80E+00	8.02E-02	1.0
1000	7.12E-01	1.38E+01	1.66E+00	1.30E-01	1.0

Appendix-III

JCPDS Data Cards for XRD Analysis

JCPDS Data Card for alpha Iron:

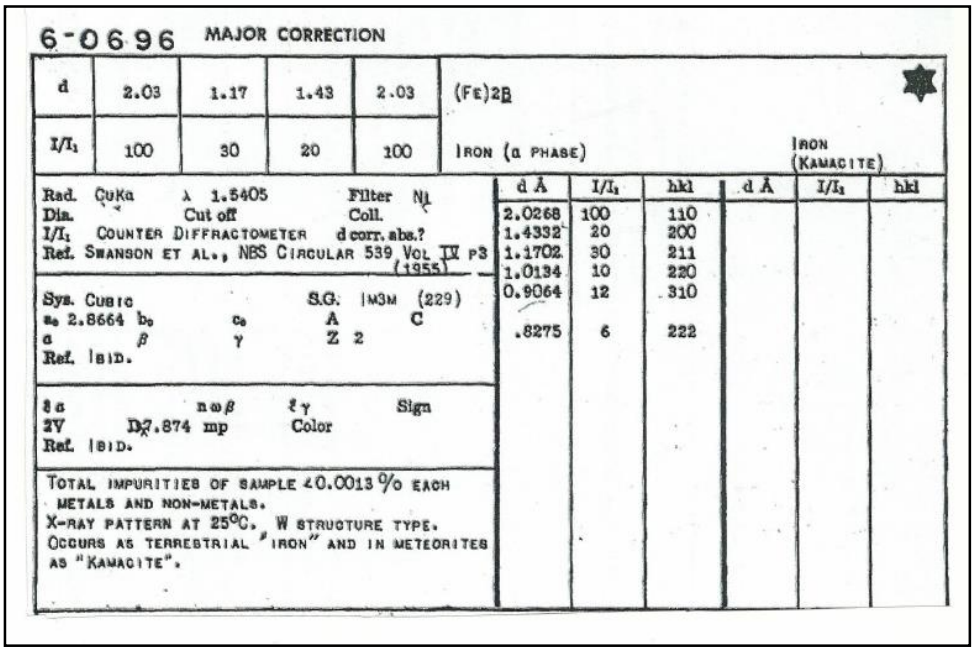

6-0696 MAJOR CORRECTION

d	2.03	1.17	1.43	2.03
I/I1	100	30	20	100

(Fe)2B

IRON (α PHASE)

IRON (KAMACITE)

Rad. CuKα λ 1.5405 Filter Ni
Dia. Cut off Coll.
I/I1 COUNTER DIFFRACTOMETER d corr. abs.?
Ref. SWANSON ET AL., NBS CIRCULAR 539 VOL IV P3 (1955)

Sys. CUBIC S.G. IM3M (229)
a0 2.8664 b0 c0 A C
α β γ Z 2
Ref. IBID.

ε α nω β ε γ Sign
2V Dx 7.874 mp Color
Ref. IBID.

TOTAL IMPURITIES OF SAMPLE <0.0013 % EACH METALS AND NON-METALS.
X-RAY PATTERN AT 25°C. W STRUCTURE TYPE.
OCCURS AS TERRESTRIAL "IRON" AND IN METEORITES AS "KAMACITE".

d Å	I/I1	hkl	d Å	I/I1	hkl
2.0268	100	110			
1.4332	20	200			
1.1702	30	211			
1.0134	10	220			
0.9064	12	310			
.8275	6	222			

JCPDS Data Card for Fe_2N:

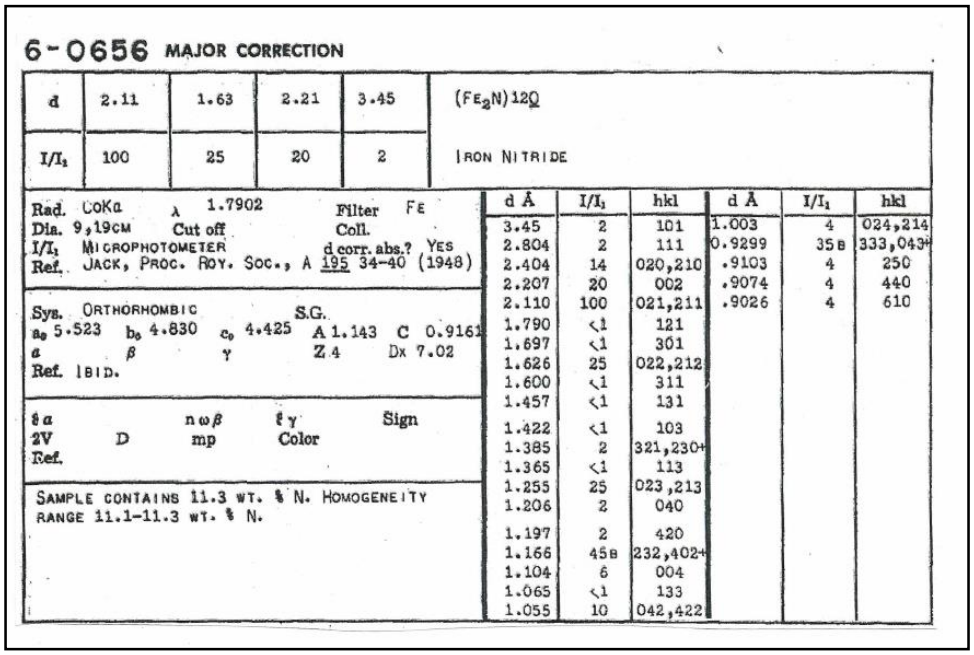

6-0656 MAJOR CORRECTION

d	2.11	1.63	2.21	3.45
I/I1	100	25	20	2

(Fe2N)12Q

IRON NITRIDE

Rad. CoKα λ 1.7902 Filter Fe
Dia. 9,19CM Cut off Coll.
I/I1 MICROPHOTOMETER d corr. abs.? YES
Ref. JACK, PROC. ROY. SOC., A 195 34-40 (1948)

Sys. ORTHORHOMBIC S.G.
a0 5.523 b0 4.830 c0 4.425 A 1.143 C 0.9161
α β γ Z 4 Dx 7.02
Ref. IBID.

ε α nω β ε γ Sign
2V D mp Color
Ref.

SAMPLE CONTAINS 11.3 WT. % N. HOMOGENEITY RANGE 11.1-11.3 WT. % N.

d Å	I/I1	hkl	d Å	I/I1	hkl
3.45	2	101	1.003	4	024,214
2.804	2	111	0.9299	3 5B	333,043
2.404	14	020,210	.9103	4	250
2.207	20	002	.9074	4	440
2.110	100	021,211	.9026	4	610
1.790	<1	121			
1.697	<1	301			
1.626	25	022,212			
1.600	<1	311			
1.457	<1	131			
1.422	<1	103			
1.385	2	321,230			
1.365	<1	113			
1.255	25	023,213			
1.206	2	040			
1.197	2	420			
1.166	45B	232,402			
1.104	6	004			
1.065	<1	133			
1.055	10	042,422			

JCPDS Data Card for Fe_3N:

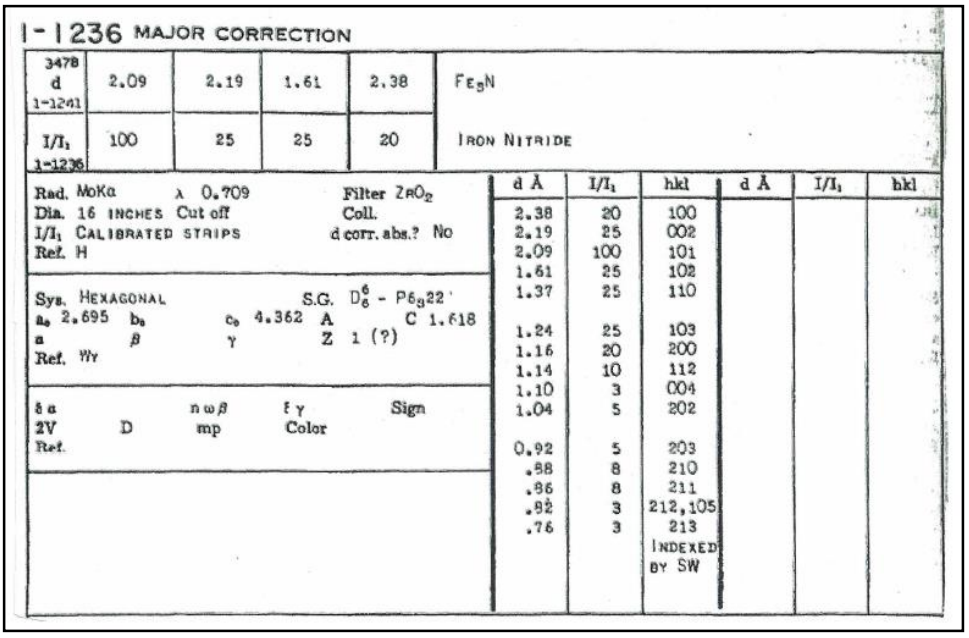

1-1236 MAJOR CORRECTION

3478 d 1-1241	2.09	2.19	1.61	2.38	Fe_3N
I/I_1 1-1236	100	25	25	20	IRON NITRIDE

Rad. MoKα λ 0.709 Filter ZrO_2
Dia. 16 INCHES Cut off Coll.
I/I_1 CALIBRATED STRIPS d corr. abs.? No
Ref. H

Sys. HEXAGONAL S.G. D_6^6 - $P6_322$
a_o 2.695 b_o c_o 4.362 A C 1.618
α β γ Z 1 (?)
Ref. Wy

δ a n ω β ε γ Sign
2V D mp Color
Ref.

d Å	I/I_1	hkl	d Å	I/I_1	hkl
2.38	20	100			
2.19	25	002			
2.09	100	101			
1.61	25	102			
1.37	25	110			
1.24	25	103			
1.16	20	200			
1.14	10	112			
1.10	3	004			
1.04	5	202			
0.92	5	203			
.88	8	210			
.86	8	211			
.82	3	212,105			
.76	3	213			
		INDEXED BY SW			

JCPDS Data Card for Fe_3N- Fe_2N:

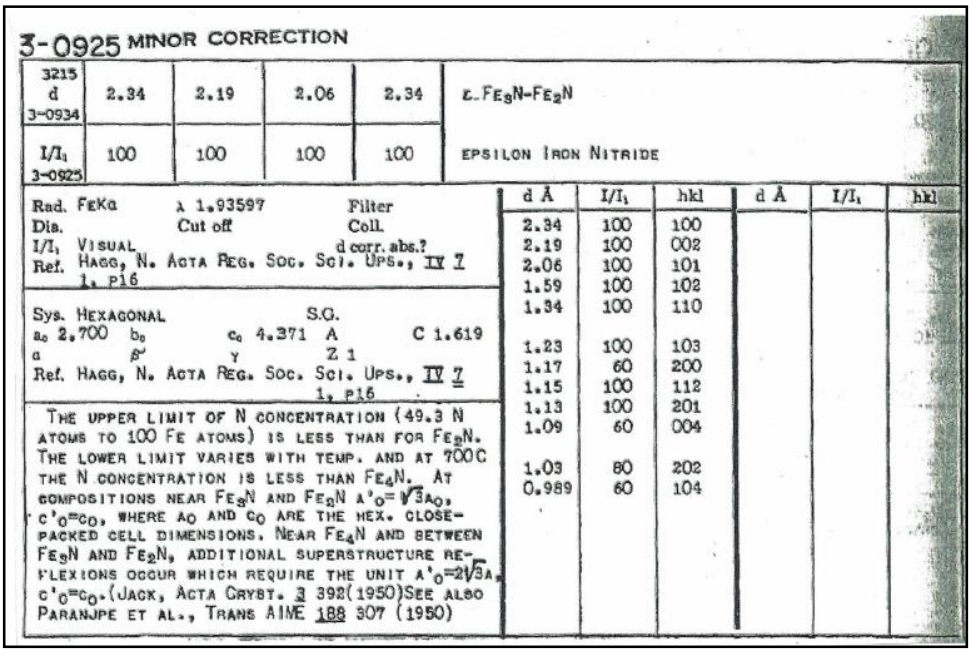

3-0925 MINOR CORRECTION

3215 d 3-0934	2.34	2.19	2.06	2.34	ε-Fe_3N-Fe_2N
I/I_1 3-0925	100	100	100	100	EPSILON IRON NITRIDE

Rad. FeKα λ 1.93597 Filter
Dia. Cut off Coll.
I/I_1 VISUAL d corr. abs.?
Ref. HAGG, N. ACTA REG. SOC. SCI. UPS., IV 7 1, P16

Sys. HEXAGONAL S.G.
a_o 2.700 b_o c_o 4.371 A C 1.619
α β γ Z 1
Ref. HAGG, N. ACTA REG. SOC. SCI. UPS., IV 7 1, P16

THE UPPER LIMIT OF N CONCENTRATION (49.3 N ATOMS TO 100 Fe ATOMS) IS LESS THAN FOR Fe_2N. THE LOWER LIMIT VARIES WITH TEMP. AND AT 700C THE N CONCENTRATION IS LESS THAN Fe_4N. AT COMPOSITIONS NEAR Fe_3N AND Fe_2N $a'_o=\sqrt{3}a_o$, $c'_o=c_o$, WHERE a_o AND c_o ARE THE HEX. CLOSE-PACKED CELL DIMENSIONS. NEAR Fe_4N AND BETWEEN Fe_3N AND Fe_2N, ADDITIONAL SUPERSTRUCTURE REFLEXIONS OCCUR WHICH REQUIRE THE UNIT $a'_o=2\sqrt{3}a$, $c'_o=c_o$. (JACK, ACTA CRYST. 3 392(1950) SEE ALSO PARANJPE ET AL., TRANS AIME 188 307 (1950)

d Å	I/I_1	hkl	d Å	I/I_1	hkl
2.34	100	100			
2.19	100	002			
2.06	100	101			
1.59	100	102			
1.34	100	110			
1.23	100	103			
1.17	60	200			
1.15	100	112			
1.13	100	201			
1.09	60	004			
1.03	80	202			
0.989	60	104			

JCPDS Data Card for Fe_4N:

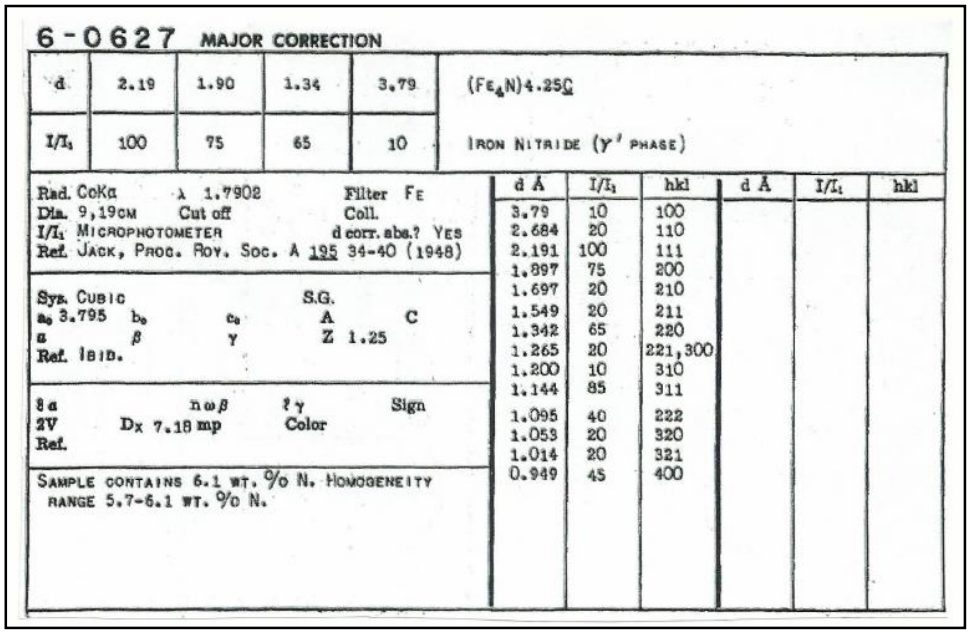

6-0627 MAJOR CORRECTION

d	2.19	1.90	1.34	3.79	$(Fe_4N)4.25C$
I/I_1	100	75	65	10	IRON NITRIDE (γ' PHASE)

Rad. CoKα λ 1.7902 Filter Fe
Dia. 9,19cm Cut off Coll.
I/I_1 MICROPHOTOMETER d corr. abs.? YES
Ref. JACK, PROC. ROY. SOC. A 195 34-40 (1948)

Sys. CUBIC S.G.
a_o 3.795 b_o c_o A C
a β γ Z 1.25
Ref. IBID.

εα nω β εγ Sign
2V Dx 7.18 mp Color
Ref.

SAMPLE CONTAINS 6.1 WT. % N. HOMOGENEITY RANGE 5.7-6.1 WT. % N.

d Å	I/I_1	hkl	d Å	I/I_1	hkl
3.79	10	100			
2.684	20	110			
2.191	100	111			
1.897	75	200			
1.697	20	210			
1.549	20	211			
1.342	65	220			
1.265	20	221,300			
1.200	10	310			
1.144	85	311			
1.095	40	222			
1.053	20	320			
1.014	20	321			
0.949	45	400			

Annexure –IV

The Finite Element Method in Solid Mechanics

1.0 Introduction

For complete description of state of stress in an object, six independent stress tensor elements are required at every point. These six stress tensor elements are related to six strain tensor elements through thirty six elastic constants in the elastic approximation of the state of deformation in the object. The six strain elements are in addition, derived from three displacement elements. For an isotropic object, the relationship between stress and strain can be described in terms of only two elastic constants (i.e. the modulus of elasticity and the Poisson ratio). On counting the number of variables at every point in the object, we find six stress tensor elements, six strain tensor elements, & three displacement vector elements. These fifteen unknown are linked through three Newtonian equations of equilibrium, six constitutive relationships between stress and strain, along with six equations connecting strain tensor elements and the displacement vector field. Thus we have a total of fifteen equations, which can be solved simultaneously along with boundary conditions to uniquely determine the stress and strain field in an object. In a generalized object of a complex geometry, these fifteen equations along with the boundary conditions are solved using either finite difference methods based on approximation theory or finite element method based on variational energy or generalized functional optimization. Thus, the FEM method is a numerical technique whose analytical foundations rest on fundamental conservation of energy principles and the application of generic variational arguments. Basis of the FEM approach for stress analysis is presented below:

2.0 The Modern FEM Based Method for Stress Analysis

2.1 Basis

For the purpose of using FEM for stress analysis of solid objects, the generalized variational principle of interest is based on the concept of virtual work for a system of volume & surface forces, as defined below:

$$\left[\partial W_{virtual} = \iiint_{\forall} \left(\hat{\phi}_V . \delta\hat{D}\right) dV + \iint_s \left(\hat{\phi}_s . \delta\hat{D}\right) dS\right] \text{-----(1)}$$

Where:

$\partial W_{virtual}$ = Variational virtual work

$\hat{\phi}_V$ = Volume force vector field

$\hat{\phi}_s$ = Surface – traction force – vector field

$[dV]$, dS = Differential volume and surface area, respectively

$[\delta\hat{D}]$ = Variational displacement vector

Using the above definition of the concept for virtual work, it can be shown that under Newtonian equilibrium, the following identity for variational quantities holds true:

$$\partial W_{virtual} = \partial U_{strain} \tag{2}$$

Where: $$\left[\left[\partial U_{strain} = \iiint_{\forall} \left(\sum_{\forall i,j} \sigma_{ij} . \delta\varepsilon_{ij} \right) dV \right]\right] \tag{3}$$

We can write Eq. (2) as:

$$\Rightarrow \delta W_{virtual} - \delta U_{strain} = 0 \tag{4}$$

$$\left[\Rightarrow \delta\left(-W_{virtual} + U_{strain}\right) = 0\right] \tag{5}$$

Now let us define:

$$-W_{virtual} = U_{Virtual} \tag{6}$$

$$\left[\Rightarrow U_{virtual} = -\iiint_{\forall} \left(\hat{\phi}_V . \hat{D}\right) dV - \iint_s \left(\hat{\phi}_s . \hat{D}\right) dS\right] \tag{7}$$

$$\Rightarrow \delta\left(U_{virtual} + U_{strain}\right) = \delta U_{total} = 0 \tag{8}$$

Finite element method divides the domains into continuous & compatible volumes (elements) and the above first variation condition is applied to each element or:

$$\left[\delta\left(\sum_{\forall i} U^{i}{}_{total}\right) = \delta(\Pi) = 0\right] \tag{9}$$

Now:

$$[\Pi = \Pi([\sigma_{ij}],[\varepsilon_{ij}],\hat{\phi}_V,\hat{\phi}_s)] \quad (10)$$

The stress tensor & the strain tensor are written in terms of a set of basis nodal displacements as below:

2.2 Transformation of Strain Tensor

$$\{a_k\} \rightarrow \{U_n\} : \{U_n\} = [N]\{a_k\} \quad (11)$$

$$\{U_n\} \rightarrow \{\varepsilon_{ij}\} : \{\varepsilon_{ij}\} = [L]\{U_n\} \quad (12)$$

$$\{\varepsilon_{ij}\} = [L][N]\{a_k\} = [B]\{a_k\} \quad (13)$$

Where:

$[N]$ = Shape function matrix

$[a_k]$ = Nodal displacement vector

$[U_n]$ = Displacement vector

$[\varepsilon_{ij}]$ = Strain tensor

2.3 Transformation of Stress Tensor

$$\{\sigma_{ij}\} = [D]\{\varepsilon_{ij}\} = [D][L][N]\{a_k\} = [D][B]\{a_k\} \quad (14)$$

Using these transformations, we can write the first variation of the total energy as:

$$\Pi = \Pi\left([B]\{a_k\},[D][B]\{a_k\},\hat{\phi}_V,\hat{\phi}_S\right) \quad (15)$$

The unknown variables, to be optimized (determined), are the basis nodal displacements $\{a_k\}$. For this we use the following detailed stationarity condition for vanishing first variation:

$$\left[\frac{\partial \Pi}{\partial \{a_k\}}\right] = \begin{bmatrix} \frac{\partial \Pi}{\partial a_1} \\ \frac{\partial \Pi}{\partial a_2} \\ \vdots \\ \vdots \\ \frac{\partial \Pi}{\partial a_m} \end{bmatrix} = \begin{bmatrix} \psi_1 \\ \psi_2 \\ \vdots \\ \vdots \\ \psi_m \end{bmatrix} = [0] \qquad (16)$$

Simultaneous solutions of the above resulting "m" simultaneous equations leads to the determination of the unknown nodal displacements from which the stress & strain state can be calculated by back-substitution in the transform equations.

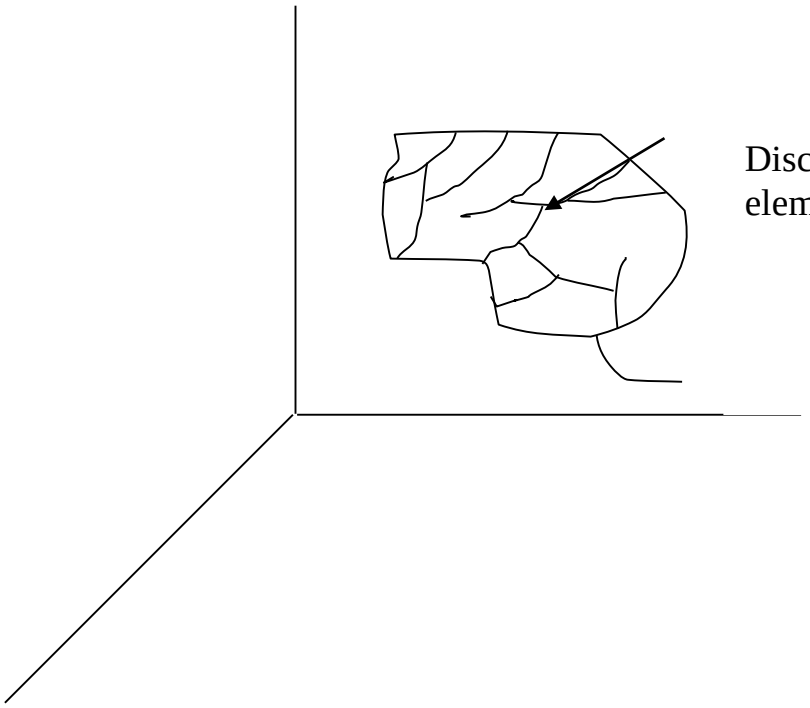

The stationarity condition results in the following equation:

$$\iiint_{\forall V} [B][\sigma] dV + [f] = [0] \qquad (17)$$

Now for isotropic solids (which is the general model used for linear elastic based FEM analysis), the following constitution equation connecting the stress tensor and the strain tensor holds:

$$\left\{\varepsilon_{ij}\right\}^{t}_{total} = \begin{bmatrix} 1/E & -\nu/E & -\nu/E & 0 & 0 & 0 \\ -\nu/E & 1/E & -\nu/E & 0 & 0 & 0 \\ -\nu/E & -\nu/E & 1/E & 0 & 0 & 0 \\ 0 & 0 & 0 & 1/2\mu & 0 & 0 \\ 0 & 0 & 0 & 0 & 1/2\mu & 0 \\ 0 & 0 & 0 & 0 & 0 & 1/2\mu \end{bmatrix} \begin{bmatrix} \sigma_{xx} \\ \sigma_{yy} \\ \sigma_{zz} \\ \sigma_{yz} \\ \sigma_{zx} \\ \sigma_{xy} \end{bmatrix}^{t^{t}}$$

$$\Longrightarrow \left\{\varepsilon_{ij}\right\}^{t}_{total} = [D]^{-1} \begin{bmatrix} \sigma_{xx} \\ \sigma_{yy} \\ \sigma_{zz} \\ \sigma_{yz} \\ \sigma_{zx} \\ \sigma_{xy} \end{bmatrix}^{t^{t}} \tag{18}$$

2.3 Computation of Invariants

Equations (17) & (18) are solved using an appropriate numerical technique and the explicit stress and strain state in each element is mapped. Once the stress state is computed, the following stress invariants can be easily computed. These invariants are connected to the dynamics of various defect structures in the object.

- **Von-Mises equivalent stress**:

$$\sigma^{2}_{Von-Mises} = \frac{1}{2}\left[(\sigma_1 - \sigma_2)^2 + (\sigma_2 - \sigma_3)^2 + (\sigma_3 - \sigma_1)^2\right]$$

(19)

- **Octahedral normal stress:**

$$\sigma_{nn} = \frac{\sigma_1 + \sigma_2 + \sigma_3}{3} \tag{20}$$

- **Octahedral shear stress:**

$$\tau_{nt} = \frac{1}{3}\left[\left[(\sigma_1 - \sigma_2)^2 + (\sigma_2 - \sigma_3)^2 + (\sigma_3 - \sigma_1)^2\right]\right] \tag{21}$$

- **Principal Shear stress:**

$$\gamma_2 = \gamma^{\max.} = \frac{|\sigma_1 - \sigma_3|}{2} \tag{22}$$

Where σ_1, σ_2, & σ_3 are the principal normal stresses (in the principal coordinate system) which can be computed by determining the three roots of the following general result for the stress tensor.

$$\det\begin{bmatrix} (\sigma_{XX} - \sigma) & \sigma_{XY} & \sigma_{XZ} \\ \sigma_{YX} & (\sigma_{YY} - \sigma) & \sigma_{YZ} \\ \sigma_{ZX} & \sigma_{ZY} & (\sigma_{ZZ} - \sigma) \end{bmatrix} = 0 \tag{23}$$

3.0 General Framework for Non-linear Solids, Non-time Invariant Solids Undergoing Irreversible Deformation (Metals, Polymers, Ceramics, & Composites)

For solids undergoing irreversible deformation, analytical techniques fall into two general categories. In category I, we have the deformation techniques wherein the state

of strain is purely dependant on the state of stress. In other words, the history of loading (loading path) and time dependant processes are not captured in the approach. While this technique is intrinsically simple, it can lead to significant errors in the final prediction of the deformed state. The category II incremental approach enables capturing of the effect of the causal time dependant loading history on the solid and enables precise predictions of the evolving state of stress and strain in the solid. In fact, the incremental approach is a superset of the deformation theory approach, as under the condition of proportional incremental loading wherein the principal stresses undergo increments in proportion to there current absolute value, the incremental approach predicts a path independent evolving state of the stress and strain in the solid similar to the deformation theory approach.

The foundations of the incremental theories rest on the pioneering work of Levy and Mises for purely plastic deformation and Prandtl&Reuss for the elastic-plastic deformation. The foundational work in the field rests on the formal approaches of Hill and Drucker who formulated a number of basic postulates, developed approaches based on plastic potential, and proved a large class of generalized mathematical results which are now widely used by designers of deformation processing techniques for materials and researchers pushing the boundaries.

With the availability of powerful parallel processor based supercomputers, ab-initio approaches based on quantum chemical modeling coupled with lattice dynamics have begun to yield very precise predictions of deformation dynamics of solids. However, this fundamental but exact approach has still not been deployed by the material forming industries who continue to rely on the continuum FEM techniques based on the mathematical approach.

The basis of the incremental framework for irreversible deformation is briefly presented below:

4.0 Incremental Elastic – Plastic Formulations for FEM Analysis

$$
\left[\begin{array}{l}
\textit{The Mathematical Machinery For The Model} \\
\bullet\ \textit{A Flow Rule} \\
F(\hat{\sigma},\kappa)=0 \text{ ------ (24)} \\
\bullet\ \textit{The Normality Condition} \\
d(\varepsilon_p)_{ij}=\lambda\dfrac{\partial F}{\partial(\sigma_p)_{ij}} \text{ ------ (25)} \\
\bullet\ \textit{The Unconstrained Normality Condition} \\
d(\varepsilon_p)_{ij}=\lambda\dfrac{\partial Q}{\partial(\sigma)_{ij}} \text{ ----(26)} \\
\textit{Where}: \\
F=\textit{Flow Rule} \\
Q=\textit{Plastic Potential} \\
\kappa=\textit{Hardening Coefficient} \\
(\varepsilon_p)_{ij}=\textit{Element of Plastic Strain Tensor} \\
(\sigma_p)_{ij}=\textit{Element of Stress Tensor} \\
\textit{Note}:\textit{When } Q=F\equiv\textit{Associated Plasticity}
\end{array}\right]
$$

Based on the above, the generalized incremental formulation for elastic-plastic problems is as below:

The Incremental Formulation

$$d(\hat{\varepsilon}_T)=d(\hat{\varepsilon}_e)+d(\hat{\varepsilon}_p)$$

$$\Rightarrow d(\hat{\varepsilon}_T)=\left[D^{-1}\right](\hat{\sigma})+\lambda\frac{\partial Q}{\partial(\hat{\sigma})} \text{ ----(27)}$$

• *Now*:

$$dF=\frac{\partial F}{\partial\sigma_1}d\sigma_1+\frac{\partial F}{\partial\sigma_2}d\sigma_2+\ldots+\frac{\partial F}{\partial\kappa}d\kappa=0 \text{ ----(28)}$$

$$\Rightarrow\left(\frac{\partial F}{\partial(\hat{\sigma})}\right)^T d(\hat{\sigma})-A\lambda=0 \text{ ----------(29)}$$

Where:

$$A\equiv-\left(\frac{\partial F}{\partial(\kappa)}\right)d\kappa\left(\frac{1}{\lambda}\right) \text{ ------(30)}$$

Combining above Equations Leads To The Formulation

$$\begin{Bmatrix} d(\hat{\varepsilon}_T) \\ 0 \end{Bmatrix} = \begin{bmatrix} D^{-1} & \dfrac{\partial Q}{\partial(\hat{\sigma})} \\ \left(\dfrac{\partial F}{\partial(\hat{\sigma})}\right)^T & -A \end{bmatrix} \begin{Bmatrix} d(\hat{\sigma}) \\ \lambda \end{Bmatrix} \text{------(31)}$$

On E lim *inating* λ, *We Can Write* :

$$d(\hat{\sigma}_T) = [D_{ep}^*] d(\hat{\varepsilon}_T) \text{--------(32)}$$

With :

$$[D_{ep}^*] = [D] - [D]\left(\frac{\partial Q}{\partial(\hat{\sigma})}\right)\left(\frac{\partial F}{\partial(\hat{\sigma})}\right)^T [D]\left[A + \left(\frac{\partial F}{\partial(\hat{\sigma})}\right)^T [D]\left(\frac{\partial Q}{\partial(\hat{\sigma})}\right)\right]^{-1} \text{---(33)}$$

5.0 Visco-plastic Problems Using the Generalized Plastic Potential Approach for FEM Analysis

Similarly, approach based on generalized plastic potential enables formulation of time dependantvisco-plastic formulation as below:

$$[\dot{\varepsilon}_{vp}] \equiv \begin{bmatrix} \dot{\varepsilon}_{vp}^1 \\ \dot{\varepsilon}_{vp}^2 \\ \vdots \\ \dot{\varepsilon}_{vp}^6 \end{bmatrix} = \gamma \langle \phi(F) \rangle \frac{\partial Q}{\partial [\sigma]} = \gamma \langle \phi(F) \rangle \begin{bmatrix} \dfrac{\partial Q}{\partial \sigma_1} \\ \dfrac{\partial Q}{\partial \sigma_2} \\ \vdots \\ \dfrac{\partial Q}{\partial \sigma_6} \end{bmatrix} \text{-----(34)}$$

$[\dot{\varepsilon}_{vp}]$ = *Six Element Strain Rate Tensor*

γ = *A Generalized Time, Temperature,* & *Total Strain Dependant Material Cons* tan *t*

ϕ = *Flow Strength Function*

F = *Plastic Triggering Flow Rule / Function*

$< > = 0$ *If* $F \le 0$

and $< > = \phi$ *If* $F > 0$

Q = *Plastic Potential*

• *The Rate Law*

$$\hat{\dot{\varepsilon}}_c = \hat{\psi}\left(\hat{\sigma}, \hat{\varepsilon}_c\right) - - - - - - - - - - (35)$$

• *Linear Strain Sum Rule*

$$\hat{\varepsilon}_{T=}\hat{\varepsilon}_e + \hat{\varepsilon}_p + \hat{\varepsilon}_c = \hat{\varepsilon}_e + \hat{\varepsilon}_c (assume\ \hat{\varepsilon}_p \equiv 0) - - - - - - (36)$$

• *Linear Elastic Solid*

$$\hat{\varepsilon}_e = \left[D\right]^{-1}\hat{\sigma} - - - - - - - - (37)$$

• *Equilibrium Equation* (*FEM Formula*)

$$\lambda \equiv \int_V \left[B\right]^T (\hat{\sigma}) dV + \left(\hat{f}\right) = 0 - - - - - - - - - (38)$$

• *In State* $(m+1)$, *We Have*:

$$\lambda_{(m+1)} \equiv \int_V \left[B\right]^T \left(\hat{\sigma}_{(m+1)}\right) dV + \left(\hat{f}_{(m+1)}\right) = 0 - - (39)$$

• *Combining Eqs.* $\Rightarrow$

$$\begin{aligned} \sigma_{(m+1)} - \sigma_{(m)} &= D\left[\varepsilon_{(m+1)} - \varepsilon_{(m)}\right] - D\left[\varepsilon_{c,(m+1)} - \varepsilon_{c,(m)}\right] \\ &= DB\left[a_{(m+1)} - a_{(m)}\right] - D\left[\varepsilon_{c,(m+1)} - \varepsilon_{c,(m)}\right] \end{aligned} \qquad - - (40)$$

• *From Creep Rate Law*:

$$\varepsilon_{c,(m+1)} - \varepsilon_{c,(m)} = \hat{\psi}_{(m+\theta)} \Delta t_{(m)} - - (41)$$

With:

$$\sigma_{(m+\theta)} = (1-\theta)\sigma_{(m)} + \theta\sigma_{(m+1)} \quad (0 \le \theta \le 1) - - - - - (42)$$

and:

$$\hat{\psi}_{(m+\theta)} = \hat{\psi}\left(\sigma_{(m+\theta)}\right) - - - - - - - - - (43)$$

• *On Combining Equations*:

$$\bar{\lambda}_{(m+1)} \equiv \sigma_{(m+1)} - \sigma_{(m)} - DB\left(a_{(m+1)} - a_{(m)}\right) + D\hat{\psi}_{(m+\theta)} \Delta t_{(m)} - - (44)$$

• *Viscoplastic Evolution* Pr*oceeds By Simul* tan*eous Solution of Eqs.*

U sin*g An Iterative Solution Scheme* (*Euler*, *Tangential*) *to Deter* min*e*:

$$a_{(m+1)}, \sigma_{(m+1)}$$